PHASE TRANSITION, DIELECTRIC AND PIEZOELECTRIC PROPERTIES OF PEROVSKITE $(Pb_{1-x}Ba_x)$ ZrO_3 CERAMICS

Naratip Vittayakorn [1,*] and Theerachai Bongkarn [2]

[1] Department of Chemistry, Faculty of Science, King Mongkut's Institute of Technology Ladkrabang, Bangkok, 10520, THAILAND
[2] Department of Physics, Faculty of Science, Naresuan University Pitsanuloke, 65000, THAILAND

ABSTRACT

$(Pb_{1-x}Ba_x)ZrO_3$ ceramics for the composition range $0 \leq x \leq 0.30$ were prepared by the mixed oxide solid state reaction method with calcination temperature at 1000°C for 1 h and sintering temperature at 1300 °C for 3 h. Structural phase and dielectric properties were studied. It was found that the density of the ceramics decreased with increasing amounts of Ba^{2+}, while the average grain size is in the range at 1 - 2.3 μm. The structure of as-calcined powder revealed that, the fraction of the orthorhombic phase decreased with increasing Ba^{2+} content. The dielectric measurement showed that the AFE-FE and FE-PE phase transformation temperatures decreased with increasing Ba^{2+} concentration. The AFE-FE phase transformation was observed for compositions $0.00 \leq x \leq 0.075$. The maximum dielectric constant gradually increases with increasing of compositions x up to 0.20. For higher Ba^{2+} concentration, the lowering of maximum dielectric values was accompanied by progressive broadening of the permittivity peak. The d_{33} values of the samples increased from ~ 0 to 87 pC/N with increasing Ba^{2+} concentration from $x = 0.000$ to 0.300.

KEYWORDS: $(Pb_{1-x}Ba_x)$ ZrO_3, Structural Phase, Phase Transformation, Dielectric Properties.

1. INTRODUCTION

Lead Zirconate, $PbZrO_3$ (PZ), is one end member of the industrially interesting solid-solution series $PbZrO_3$-$PbTiO_3$ [1] and the first antiferroelectric identified by Sawaguchi *et al.* [2,3]. At room temperature PZ is an antiferroelectric phase (AFE) which has an orthorhombic structure [2]. It undergoes the AFE to a paraelectric phase (PE) and transforms from the orthorhombic structure to a cubic structure at 236°C [4]. It was reported that PZ exist a ferroelectric phase (FE) over a very narrow temperature range (230-233 °C) [5-8]. The FE intermediate phase can be also introduced by partial replacement of Pb^{2+} ions with Ba^{2+} ions. The temperature range of this intermediate phase also increases with the Ba concentration [9-16]. The AFE-FE phase transition produced a large volume expansion. It makes this material potentially useful for high displacement electromechanical actuator applications [15,16].

Effects of Ba^{2+} ions substitution on the phase transformation behavior of PZ has been investigated by many authors [4,9-21]. Roberts is the first person who studied of this behaviors but he did not get any evidence of the AFE to FE transformation [4]. Later, Shirane investigated the phase transformation behavior of $(Pb_{1-x}Ba_x)ZrO_3$ (PBZ) for $0 \leq x \leq 0.30$ and reported that the ferroelectric intermediate phase did not appear until Ba^{2+} concentration exceeded the threshold value at about 5 mol% [9]. The temperature range of this intermediate phase increased with the Ba^{2+} concentration. On the contrary, Ujma *et al.* reported the FE phase existence in PBZ containing up to 5 mol% Ba^{2+}, which found that dielectric properties were differed from the previous papers [17]. Harrad *et al.* had carried out in details from a Raman scattering study of phase transformations in PBZ ceramics and shown that the AFE phase persisted up to a critical composition of $x = 0.175$ [18,19]. Recently, Pokharel *et al.* synthesized PBZ by semiwet route to ensure a homogeneous distribution of Pb^{2+} and Ba^{2+}[14-17,20,22]. They found unusual wide thermal hysteresis in the transformation temperatures measured by dielectric during heating and cooling cycles (e.g., nearly 100 °C for $x = 0.05$ in contrast to about 11 °C for pure PZ) and irreversibility of the AFE to FE transformation temperature during cooling cycle for $x = 0.10$.

* Corresponding author.
E-mail: naratipcmu@yahoo.com

However, the dielectric properties measured on cooling cycle of PBZ ceramics which prepared via mixed oxide solid state method has not been performed. Moreover, microstructure and piezoelectric properties of PBZ system have not been clearly understood. In this present work, $(Pb_{1-x}Ba_x)ZrO_3$ (PBZ) for $0 \leq x \leq 0.30$ were prepared by solid state reaction method. Structural phase, densification, microstructure and piezoelectric properties of PBZ ceramics are investigated as a function of compositions x. Permittivity measurements are also used for study the details of antiferroelectric (AFE) to ferroelectric (FE) and ferroelectric (FE) to paraelectric (PE) phases transformations accompanied with evaluations of dielectric behaviors of PBZ samples. The results are discussed and compared to the previous works.

2. EXPERIMENTAL PROCEDURE

The $(Pb_{1-x}Ba_x)ZrO_3$, $0 \leq x \leq 0.30$, ceramics were prepared by using a conventional mixed oxide method. The raw materials of PbO, ZrO_2 and $BaCO_3$ were weighed and mixed. Each mixture of the starting powders was milled and mixed in a ball mill, as well as wet-homogenized with acetone for 24 h using zirconia grinding media. The suspensions were dried and the powders were ground using an agate mortar and sieved in to fine powder. All obtained powders were calcined at 1000 °C for 1 h. The calcined powders were reground by wet ball-milling with 1wt% binder (B-5 supplied by Rohn-Haas, Germany) for 24 h. After grinding and sieving, 5 wt% of polyvinyl alcohol (PVA) binder was added. Discs with a diameter of 1.5 cm were prepared by cold uniaxial pressing at a pressure of 150 MPa. Finally, the discs were sintered in a sealed alumina crucible at temperatures 1300°C using a heating rate of 5°C/min and a dwell time of 3 hours. In order to minimize the loss of lead due to vaporization, the PbO atmosphere for the sintering was maintained using $PbZrO_3$ as the spacer powder. The microstructures of the sintered samples were examined using a scanning electron microscopy (JEOL, JSM5910). The phase formation of the calcined powders was determined using a diffractometer (Philips ADP1700). The density of the sintered samples was measured by Archimedes' method with distilled water as the fluid medium. The sintered samples were prepared for electrical property measurements by first polishing and then gold sputtering on to the clean pellet faces. The poling was done conventionally, in silicone oil bath at 170 °C with a field of 25 kV/cm. After poling, the d_{33} coefficient was measured using a d_{33} tester (Pennebaker Model 8000). The dielectric measurements were carried out at 1 kHz using a HIOKI 3532-50 impedance analyzer, from room temperature to 300 °C with a heating and cooling rate of 0.5 °C/min controlled by a computer.

3. RESULTS AND DISCUSSION

XRD patterns of the calcined $(Pb_{1-x}Ba_x)ZrO_3$ powders for $0.000 \leq x \leq 0.300$ are shown in Fig. 1. Other than the perovskite, phase was not observed for the whole range of compositions. Also the XRD patterns indicate that the replacement of Pb^{2+} by Ba^{2+} ions apparently influenced the orthorhombic $PbZrO_3$ structure. For all of the samples, the diffraction lines could be indexed with respect to an orthorhombic structure. The intensity ratio of 004/240 peaks and the relative intensity of superlattice reflections, namely 110 and 130/112 are decreased with increasing of Ba^{2+} content. Pokharel *et al.* reported that the XRD pattern of orthorhombic antiferroelectric (A_O) phase presents the doublet of 240 and 004 reflections change to the single peak of 200 reflections for rhombohedral ferroelectric (F_R) phase [14-17]. For a purely orthorhombic pattern, $I_{004/240} \sim 0.5$ and this value decreases with increasing amounts of coexisting rhombohedral phase. In addition, the superlattice reflections, such as 110 and 130/112 of A_O phase, are absolutely disappeared for the F_R phase. Therefore, the structure of as-calcined powder also revealed that, the fraction of the orthorhombic phase is decreasing with increasing Ba^{2+} content.

Fig. 2 shows the typical sintered densities for various PBZ compositions. The bulk densities for all samples are higher than 97% of theoretical density. The bulk density continuously decreases with increasing Ba^{2+} content. These result are in good agreement with those reported by Pokharel *et al.* [17]. In general, the bulk density of $PbZrO_3$-$BaZrO_3$ system decreased with increased mol percent of $BaZrO_3$ (BZ). The theoretical density of the constituent compounds PZ and BZ are 8.055 and 6.229 g/cm^3, respectively [23,24], which can be used to calculate an empirical estimate of the density (D) via the equation:

$$D = ((1-x) \times 8.055) + (x \times 6.229) \quad (1)$$

The variation of the measured density and the calculated density with composition x is also shown in Fig. 2.

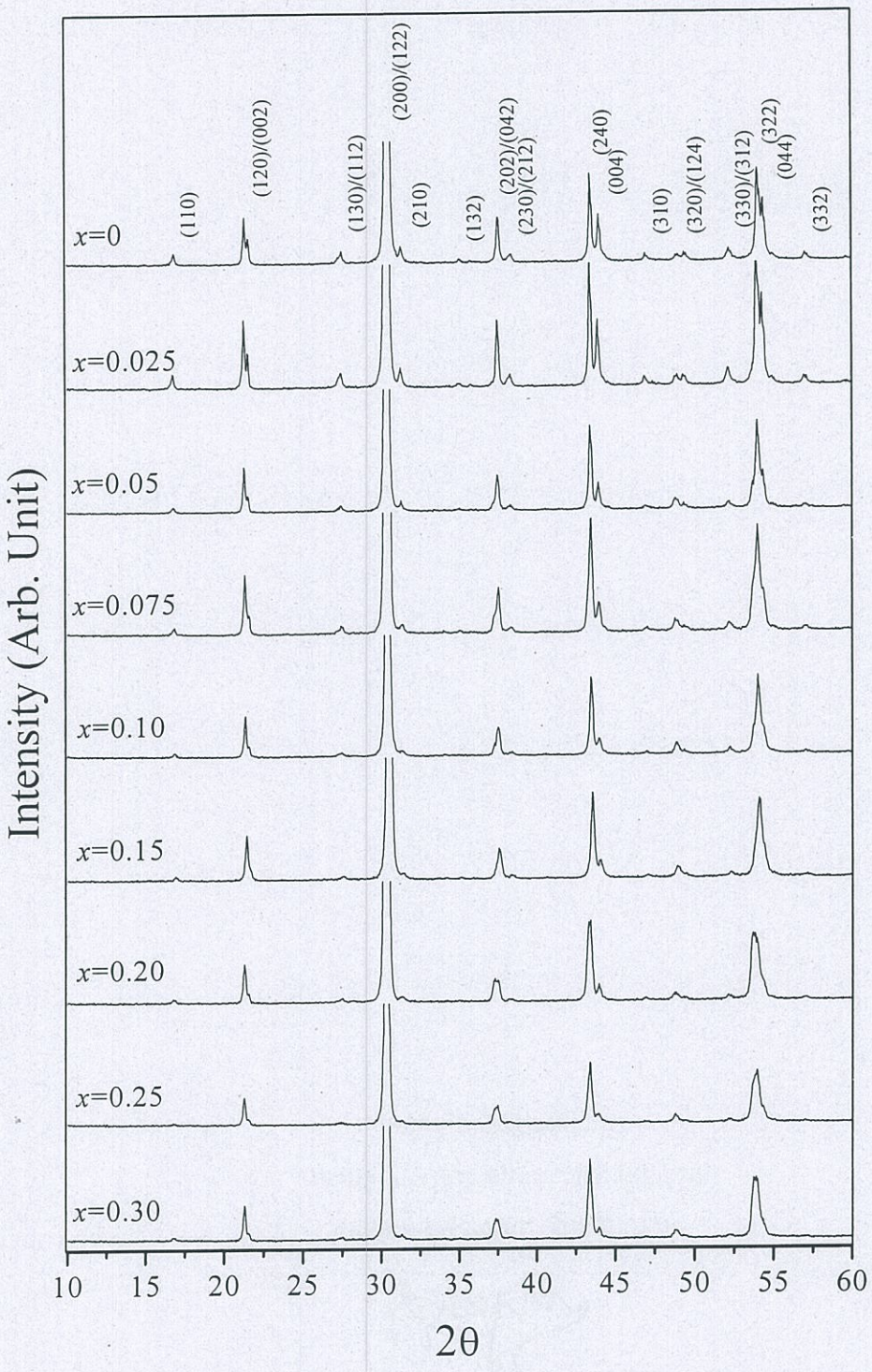

Fig. 1 XRD patterns of calcined powders of $(Pb_{1-x}Ba_x)\ ZrO_3$.

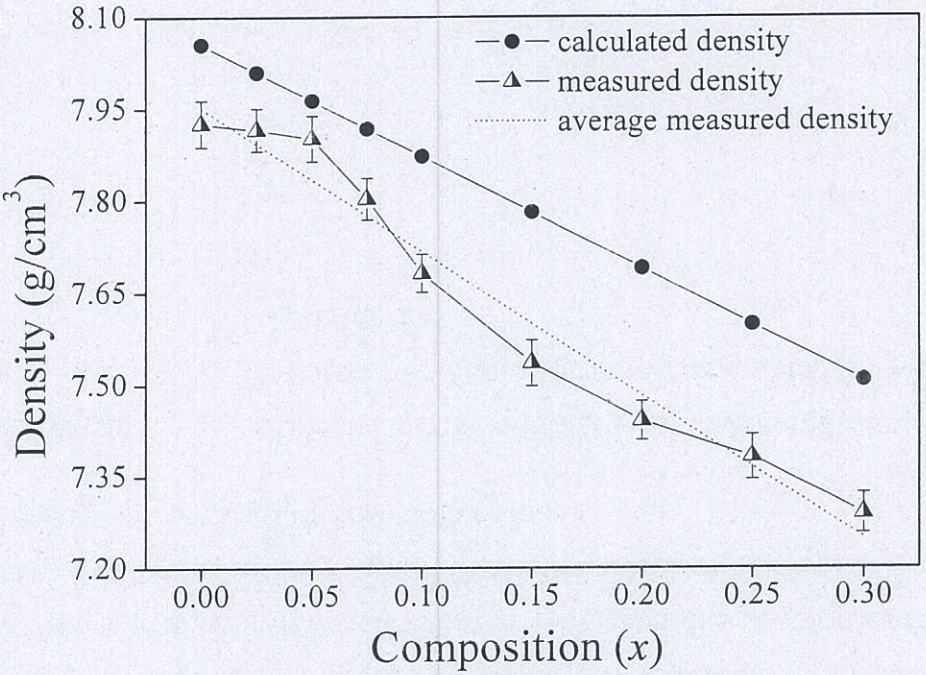

Fig. 2 Calculated density and bulk density of sintered pellets as a function of composition x.

The scanning electron micrographs in Fig. 3 show the as-sintered surface of $(Pb_{0.950}Ba_{0.050})ZrO_3$ and $(Pb_{0.800}Ba_{0.200})ZrO_3$ ceramics. It can be seen that the samples with higher Ba^{2+} concentration show high uniformity in grain size. Particle size can be estimated from SEM micrographs to be in the range of 1-2.3 μm. Fig 4 depicts the variation of dielectric constant with temperature during heating and cooling of samples for $0 \leq x \leq 0.30$. By replacing lead with barium, the dielectric maximum of lead zirconate is shown to be shifted to lower temperature. On heating the anomalies around 193, 157, and 116 °C for x = 0.025, 0.050 and 0.075, respectively, were found. These anomalies are due to transformation from the A_O phase to F_R phase [9,13,25]. While the dielectric maximum on heating in all samples, is linked with the transformation of the F_R phase into the P_C phase [9,13,25].

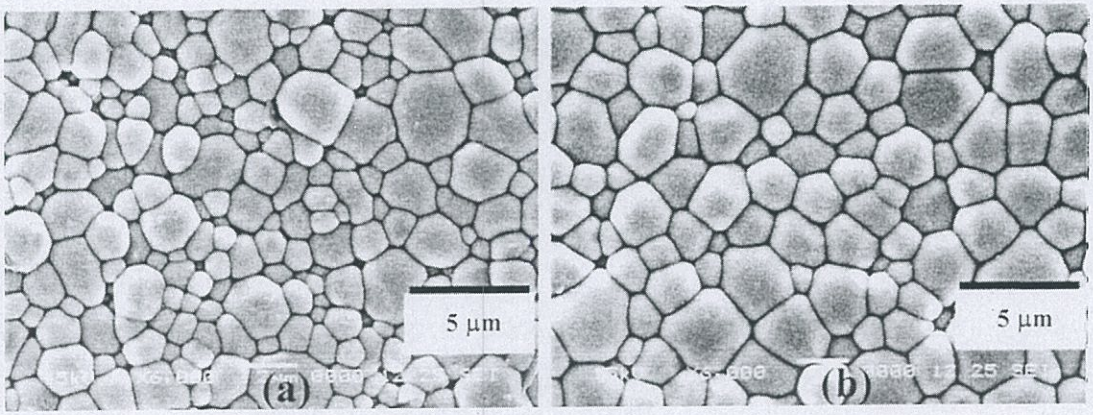

Fig. 3 SEM micrographs of as-sintered surface of (a) $(Pb_{0.950}Ba_{0.050})ZrO_3$ and (b) $(Pb_{0.800}Ba_{0.200})ZrO_3$ ceramics.

The AFE to FE transformation of PZ can not be observed during heating, as shown in Fig. 4. The absence of phase transformation may be due to some impurities from raw materials [6,26]. The FE

to AFE transformation during cooling occurs at 194 °C. This anomaly can be seen from dielectric loss curve, which made possible accurate determination from temperatures of phase transformation between the AFE and FE phase [12,27]. The intermediate FE phase of PZ existed only on cooling cycle and agrees with previous works [28-30]. However, the FE to AFE transformation temperature in this study is lower than the former works. The reason for lower FE to AFE transformation temperature of PZ is not clear now.

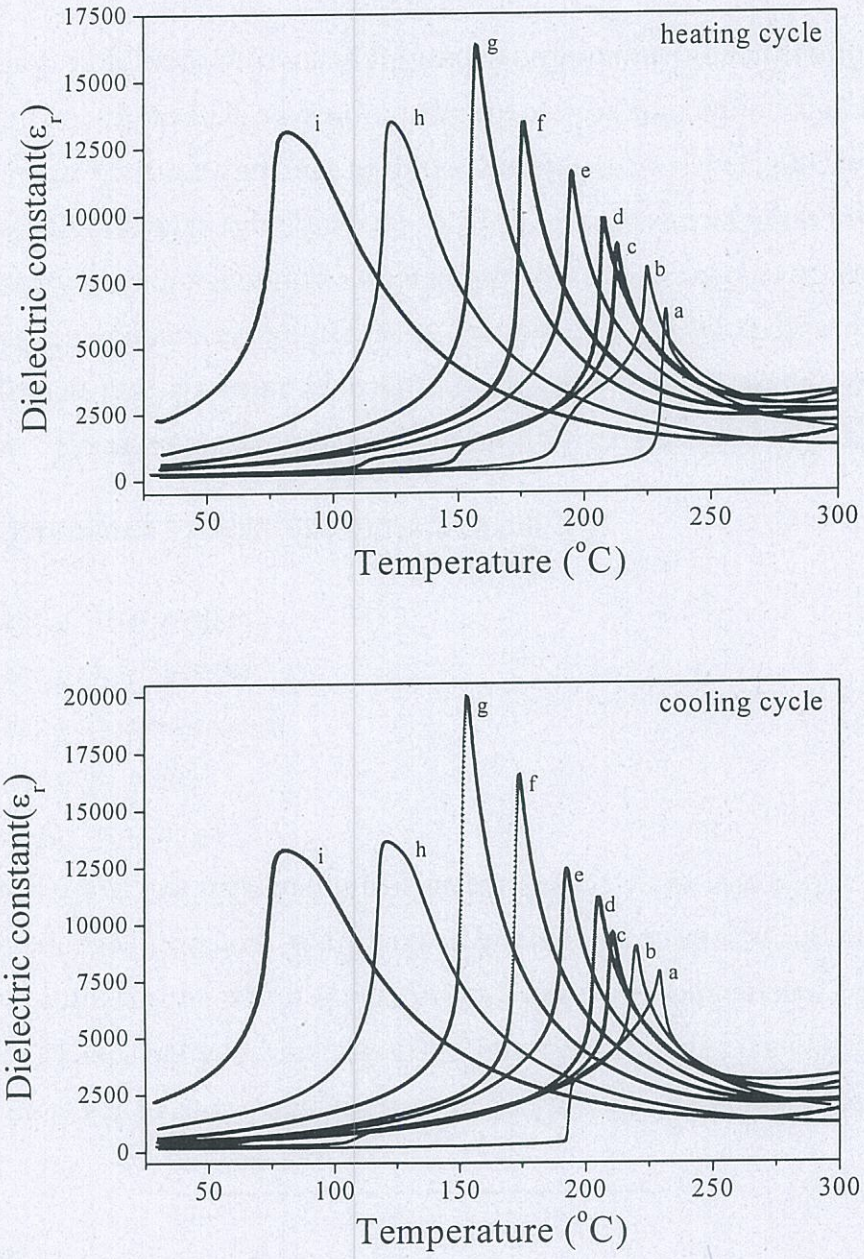

Fig. 4 Dielectric constant versus temperature on heating and cooling cycle of $(Pb_{1-x}Ba_x)ZrO_3$ ceramics; (a) x=0, (b) x=0.025, (c) x=0.05, (d) x=0.075, (e) x=0.10, (f) x=0.15, (g) x=0.20, (h) x=0.25, (i) x=0.30.

For $x \geq 0.10$, no dielectric anomaly corresponding to the AFE to FE transformation is observed either in the temperature variation of the dielectric constant or in the temperature variation of

dielectric loss. It can be noted that the AFE to FE transformation temperature decreases nearly linearly at the rate of ~ 16 °C/mol% of $BaZrO_3$ with respect to its value for pure PZ.

The transformation temperatures for heating and cooling cycles for PBZ2.5 are 191 °C and 110 °C respectively while those for PBZ5 are 155 and 70 °C, respectively. For PBZ2.5 and PBZ5, the jump of the dielectric constant during the cooling cycle is 650 and 530, which is considerably lower than the value of 2010, 1430 for the heating cycle, respectively. The situation becomes more anomalous for PBZ7.5 for which one observes a dielectric anomaly during the heating cycle only but not during the cooling cycle as can be noted from the temperature variation of dielectric constant and of dielectric loss. This result similar to what has been reported by Pokharel *et al.*, in the dielectric measurement for $(Pb_{0.90}Ba_{0.10})ZrO_3$ [14,15]. This indicates that the AFE to FE transformation is not reversible during the cooling cycle. The quenching of the FE phase to room temperature during cooling cycle has been further confirmed by the absence of the dielectric anomaly corresponding to the AFE to FE transformation when the sample was again heated after the cooling cycle. As shown elsewhere, the AFE phase eventually reappears from the metastable FE matrix on aging the sample at room temperature but the kinetics of the recovery is extremely sluggish and may require several months [14]. In the present work, the thermal hysteresis of AFE-FE phase transformations is about 80 and 100 °C for composition of x = 0.025 and 0.050, respectively. The width of temperature range of F_R phase on heating is 32.6, 56.7 and 92.3 °C for composition of x = 0.025, 0.050 and 0.075, respectively, while on cooling is 35.5, 110.0 and 143.3 °C for composition of x = 0.00, 0.025 and 0.050, respectively.

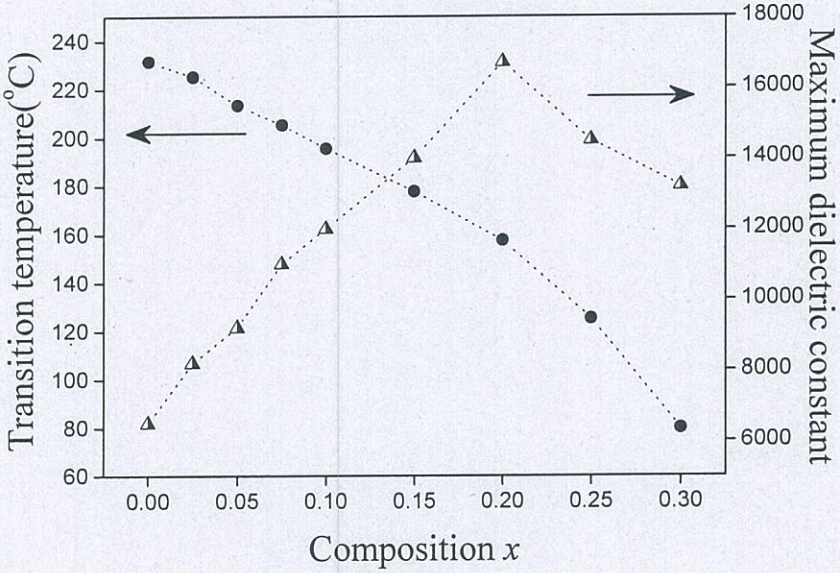

Fig 5. Transition temperature and maximum dielectric constant as a function of composition x at 1 kHz

The FE phase of pure PZ transforms into the PE phase occurs at 232 °C during heating cycle. There is a hysteresis of about 3 °C in the transformation temperatures obtained during heating and cooling cycles confirming the first order nature of this transformation for pure PZ [6,8,15]. The increasing amount of Ba^{2+} is accompanied by a decrease in the transformation temperature. Barium substitution at the Pb^{2+} site increases the room temperature dielectric constant from 160 for pure PZ to nearly 2300 for PBZ30. The value of the dielectric constant at the FE to PE phase transformation temperature during heating cycle increases with increasing Ba^{2+} content from 6300 for pure PZ to 16300 for PBZ20 (x = 0.20). For higher Ba^{2+} concentration, the lowering of maximum dielectric values is accompanied by the progressive broadening of the permittivity peak. The increase in dielectric constant related to the change of the PBZ structure, may facilitate the parallel displacement along a [111] direction and the associated displacement of three oxygen ions in the PBZ structure, resulting in an improvement of ferroelectricity. The presence of a polar axis in the [111] direction has been reported for a ferroelectric rhombohedral structure [12]. However, above 25 and 30 mol% Ba^{2+} composition, a slight decrease in the maximum dielectric constant was observed. As shown in Fig. 4, the Curie temperature shifted to a lower temperature linearly, which may be explained by the increase of symmetry in the PBZ structure with increasing Ba^{2+} ions as previous mentioned and this system is a

well behaved complete solid solution. The maximum permittivity $\varepsilon_{r,max}$ and T_{max} as a function of the mole fraction of $Ba^{2+}(x)$ are represented in Fig. 5. These results are similar to those reported in the earlier papers [9,13]. However, in this study, the specimens exhibited a higher dielectric constant than earlier papers [4,9,14,15]. This feature is probably due to better conditions for the sinter process then the dense and homogeneous samples were achieved. The difference in the transformation temperatures obtained during heating and cooling measurements for $0.050 < x < 0.30$ remains nearly the same as for pure PZ (i.e., 3 °C) confirming that the FE to PE transformation over the entire composition range ($0 < x < 0.30$) is first order.

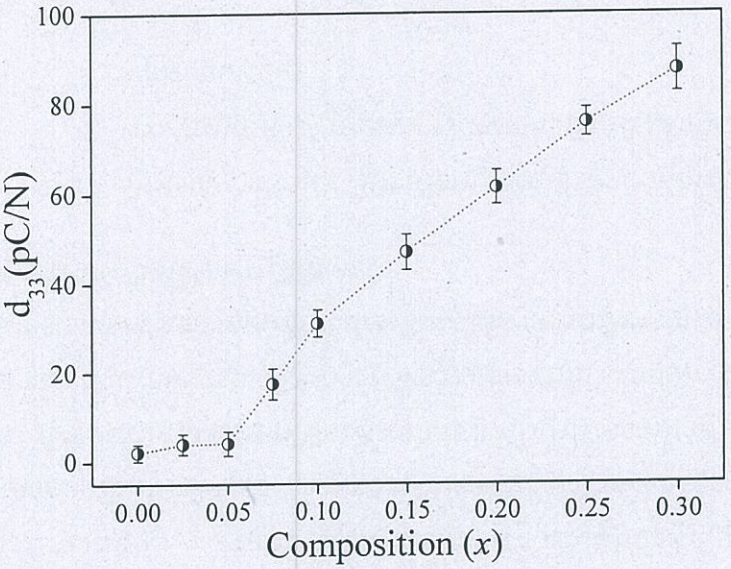

Fig. 6 Piezoelectric coefficient d_{33} and dielectric constant at room temperature of $(Pb_{1-x}Ba_x)ZrO_3$ with various x.

The longitudinal piezoelectric sensitivity of $(Pb_{1-x}Ba_x)ZrO_3$ at room temperature are shown in Fig. 6. The d_{33} value gradually increases with increasing Ba^{2+} content. Roberts [4] reported that the d_{33} value of $(Pb_{0.700}Ba_{0.300})ZrO_3$ was ~ 65 pC/N, and it is 10^{-1} pC/N for PZ [27]. The present result indicated that substitution of Ba^{2+} for Pb^{2+} enhanced some piezoelectric property in PBZ.

4. CONCLUSIONS

In the present work, effect of Ba^{2+} concentration on the properties of the PBZ ceramics was studied. The orthorhombic phase and the fraction of the antiferroelectric phase were found to decrease with increasing Ba^{2+} content. The results were corresponded to the structural phase changes in PBZ. The bulk density of PBZ ceramics continuously decreases with increasing Ba^{2+}content. This trend matches with the calculated density of the PZ-BZ system. The d_{33} value at room temperature gradually increases with increasing Ba^{2+} content. Furthermore, the results indicated that Ba^{2+} concentration has a significant effect on the dielectric properties in PBZ ceramics. The AFE-FE and FE-PE phase transformation temperatures progressively decreases with continuously increasing Ba^{2+} concentration. The AFE-FE phase transformation is detected for compositions $0.00 \leq x \leq 0.075$.

ACKNOWLEDMENT

This work was supported by Thailand Research Fund (TRF), Faculty of Science, Naresuan University and King Mongkut's Institute of Technology, Ladkrabang, Thailand.

REFERENCES

[1] Ainger F.W. **1972** *Modern Oxide Materials*, Academic Press, New York, pp. 147-175.

[2] Sawaguchi E., Shirane G., Hoshino S. **1951** Antiferroelectric Structure of Lead Zirconate *Physical. Review,* 83, 1078.

[3]. Sawaguchi E., Shirane G., Takagi Y. **1951** Phase Transition in Lead Zirconate *Journal of the Physical Society of Japan* 6, 333-339.

[4] Roberts S. **1953** Dielectric properties of lead zirconate and barium lead zirconate, *Journal of the American Ceramic Society* 33, 63-66.

[5] Goulpeau L. **1967** *Sov. Phys. Solid St.* 8, 1970-1971.

[6] Tennery V.J. **1966** High-temperature phase transitions in $PbZrO_3$ *Journal of the American Ceramic Society* 49, 483-486.

[7] Scott B.A., Burns G. **1972** Crystal growth and observation of the ferroelectric phase of $PbZrO_3$ *Journal of the American Ceramic Society* 55, 331-333.

[8] Whatmore R.W., Glazer A.M. **1979** Structural phase transitions in lead zirconate *Journal of Physics C: Solid State Physics.* 12, 1505-1516.

[9] Shirane G. **1952** Ferroelectricity and Antiferroelectricity in Ceramic $PbZrO_3$ Containing Ba or Sr, *Physical. Review* 86, 219-227.

[10] Shirane G., Hoshino S. **1954** X-ray study of phase transitions in $PbZrO_3$ containing Ba or Sr *Acta Crystallographica* 7, 203-210.

[11] Yamakawa K., Trolier-McKinstry S., J. P. Dougherty and Krupanidhi S. B. **1995** Reactive magnetron co-sputtered antiferroelectric lead zirconate thin films, *Applied Physics Letters* 67(14), 2014-2016.

[12] Ujma Z., Handerak J., Pawelczyk M., Dmytrow D. **1992** Phase composition and dielectric properties of lead barium zirconate solid solutions, *Ferroelectrics* 129,127-139.

[13] Yoon K.H. , Hwang S.C. **1997** Dielectric and field-induced strain behaviour of $(Pb_{1-x}Ba_x)\ ZrO_3$ ceramics *Journal of Materials Science*, 32, 17-21.

[14] Pokharel B. P., Pandey D. **1999** Irreversibility of the antiferroelectric to ferroelectric phase transition in $(Pb_{0.90}Ba_{0.10})ZrO_3$ ceramics *Journal of Applied Physics*, 86, 3327-3332.

[15] Pokharel B.P., Pandey D. **2000** Dielectric studies of phase transitions in $(Pb_{1-x}Ba_x)ZrO_3$ *Journal of Applied Physics*. 88, 5364-5373.

[16] Pokharel B.P., Pandey D. **2001**High temperature x-ray diffraction studies on antiferroelectric and ferroelectric phase transitions in $(Pb_{1-x}Ba_x)ZrO_3$ (x = 0.05,0.10) *Journal of Applied Physics,* 90, 2985-2294.

[17] Pokharel B. P., Datta M. K., Pandey D. **1999** Influence of calcination and sintering temperatures on the structure of $(Pb_{1-x}Ba_x)ZrO_3$ *Journal of Materials Science* 34, 691-700.

[18] El-Harrad I., Becker P., Carabatos-Nedelec C., Handerek J., Ujma Z., Dmytrow D. **1996** Raman scattering investigation with temperature of the phase transitions in $(Pb_{0.825}Ba_{0.175})ZrO_3$ and $(Pb_{0.65}Ba_{0.35})ZrO_3$ ceramics, *Vibrational Spectroscopy* 10, 301-309.

[19] El-Harrad I., Ridah A., Carabatos-Nedelec C., Becker P., Handerek J., Ujma Z., Dmytrow D. **1998** Raman scattering investigation with temperature of phase transitions in $(Pb_{1-x}Ba_x)ZrO_3$ ceramics at critical compositions x=0.175 and 0.35,*Journal of Raman Spectroscopy* 29, 123-129.

[20] El-Harrad I., Ridah A. **2002** Charge Transfer Vibronic Excitons in Incipient Ferroelectrics and Related Problems, *Ferroelectrics* 265, 211-223.

[21] Pokharel B. P., Ranjan R., Pandey D. **1999** Rhombohedral superlattice structure and relaxor ferroelectric behavior of $(Pb_{0.70}Ba_{0.30})ZrO_3$ ceramics *Applied Physics Letter* 74, 756-758.

[22] Pokharel B. P., Pandey D.**2002** Effect of Ba^{2+} substitution on the stability of the antiferroelectric and ferroelectric phases in $(Pb_{1-x}Ba_x)ZrO_3$: Phenomenological theory considerations *Physical. Review B* 65, 214108.

[23] Powder Diffraction File no.87-0570, International Centre for Diffraction Data, Newton Square, PA, 2000.

[24] Powder Diffraction File no.06-0399, International Centre for Diffraction Data, Newton Square, PA, 2000.

[25] Debretteville A. P. **1954** Threshold Field and Free Energy for the Antiferroelectric-Ferroelectric Phase Transition in Lead Zirconate *Physical. Review* 94, 1125-1128.

[26] Handerek J., Pawelczyk M., Ujma Z. **1981** The influence of an electric field and hydrostatic pressure on dielectric properties and phase transitions in $PbZrO_3$ *Journal of Physics C: Solid state Physics* 14, 2007-2016.

[27] Roberts S. **1951** Polarizabilities of Ions in Perovskite-Type Crystals *Physical. Review* 81, 865.

[28] Tani T., Li J-F., Viehland D., and Payne D. A. **1994** Antiferroelectric-ferroelectric switching and induced strains for sol-gel derived lead zirconate thin layers *Journal of Applied Physics* 75(6), 3017-3023

[29] Ujma Z., Handerek J. **2003** Peculiarities of the pyroelectric effect and of the dielectric properties in Bi-doped $Pb(Zr_{0.95}Ti_{0.05})O_3$ ceramics *Journal of the European Ceramic Society* 23, 203-212.

[30] Belov A. A., Jeong Y. **1998** Anomalous Thermal Hysteresis in the Dielectric Constant of $PbZrO_3$ *Journal of the Korean Physical Society* 32, S299-S301.